Structurally different mono, bi and trinuclearPd(II) complexes and their DNA/Protein interaction, DNA cleavage, anti-oxidant, anti-microbial and cytotoxic studies

A. Shanmugapriya,[a]RuchiJain,[b]D. Sabarinathan,[c]G. Kalaiarasi,[a] F. Dallemer[d] and R. Prabhakaran[a*]

Experimental

4. 2.DNA binding studies

The experiments involving CT-DNA were performed in double distilled water with tris(hydroxymethyl)aminomethane (Tris, 5 mM) and sodium chloride (50 mM) and adjusted to pH 7.2 with hydrochloric acid. The concentration of CT-DNA was determined by UV absorbance at 260 nm. The molar absorption coefficient, $\varepsilon_{max}260$, was taken as 6600 M^{-1} cm^{-1}.[6] CT-DNA solution of various concentrations (0.5-5 μM) dissolved in Tris-HCl (pH 7.2) were added to the palladium complexes **1-4** (10 μM dissolved in a DMSO-H_2O mixture). Absorption spectra were recorded after equilibrium at 20 ºC for 10 min. The intrinsic binding constant K_b was determined by using the Stern-Volmer equation (1).[1]

$$([DNA] / [\text{Ɛ}_a - \text{Ɛ}_f]) = [DNA] / [\text{Ɛ}_b - \text{Ɛ}_f] + 1/ K_b[\text{Ɛ}_b - \text{Ɛ}_f] \qquad (1)$$

The absorption coefficients Ɛ_a, Ɛ_f, and Ɛ_b correspond to A_{obsd}/[DNA], the extinction coefficient for the free complexes and the extinction coefficient for the complexes in the fully bound form, respectively. The intrinsic binding constant K_b can be obtained from the ratio of the slope to the intercept in plots of [DNA]/ $[\text{Ɛ}_a - \text{Ɛ}_f]$ versus [DNA].

4.2.1 Competitive binding with ethidium bromide

To find out the exact mode of attachment of CT-DNA to the complexes, fluorescence quenching experiments of EB-DNA were carried out by adding 10 μL portion of 10 μM palladium(II) complexes every time to the sample containing 10 μM EB, 10 μM DNA and Tris buffer (pH 7.2). Before the measurements, the system was shaken and incubated at room temperature for ~5 min. The emission spectra were recorded at 530-750 nm. On the basis of the classical Stern-Volmer equation, the quenching constant has been analysed (2).

$$I_0/I = K_{sv}[Q] + 1 \qquad (2)$$

Where I_0 and I represent the emission intensities in the absence and presence of the complexes, respectively, K_{sv} is the quenching constant, and [Q] is the concentration ratio of the complex. The K_{sv} values have been obtained as a slope from the plot of I_o/I versus [Q].

Further, the apparent DNA binding constant (K_{app}) were calculated using the following equation,

$$K_{EB}\,[EB] = K_{app}[complex]$$

(Where [complex] is the value at a 50% reduction in the fluorescence intensity of EB, K_{EB} ($1.0 \times 10^7\ M^{-1}$) is the DNA binding constant of EB, [EB] is the concentration of EB =10 μM).

4.2.2 DNA cleavage studies

The cleavage of DNA was monitored by using agarose gel electrophoresis. Supercoiled pBR322 DNA (100 mg) in 5% DMSO and 95% Tris buffer (5 mM, pH 7.2) with 50 MmNaCl was incubated at 37°C in the absence and presence of compounds. The DNA, compound and sufficient buffer were premixed in a vial, and the reaction was allowed to proceed for 2 h at 37°C. The samples were then analyzed by 1.5% agarose gel electrophoresis in tris-acetic acid-ethylenediaminetetraacetic acid buffer. The gel was stained with 0.5 μg cm^{-3}ethidium bromide before migration. After electrophoresis at 50 V for 3 h, the gel was illuminated and the digital images were analyzed by gel documentation system (SYNGEN USA).[2]

4.3 Bovine serum albumin binding study

BSA solution(10 μM) was prepared in phosphate buffer of pH 7.2 and stored in the dark at 4 °C for use. The excitation wavelength of BSA at 280 nm and the emission at 346 nm were monitored for the protein binding studies. The excitation and emission slit widths and scan rates were maintained constant for all of the experiments. Concentrated stock solution of complexes were prepared by dissolving the compounds in DMSO and diluted suitably with deionised water to required concentrations for all the experiments (1% DMSO in the final solution). Quenching of the emission intensity of tryptophan residues of BSA at 346 nm (excitation wavelength at 276 nm) was monitored using compound as quenchers with increasing compound concentration. The possible quenching mechanism has been interpreted using the Stern-Volmer equation (2).

When small molecule bind to the active site of BSA, the equilibrium binding constant and the number of binding sites can be analysed by using the Scatchard equation (4).

$$\log[F_0 - F/F] = \log K + n \log[Q] \qquad (4)$$

Where K is the binding constant of quencher with BSA, n is the number of binding sites, F_0 and F are the fluorescence intensity in the absence and the presence of the quencher. Which can be determined by the slope and the intercept of the double logarithm regression curve of log $[(I_0-I)/I]$ versus log[Q]. Synchronous fluorescence spectra of BSA with various concentrations of complexes (0-100 μM) were obtained from 300 to 500 nm when $\Delta\lambda$= 60 nm and from 290 to 500 nm when$\Delta\lambda$ = 15 nm. The excitation and emission slit widths were 5 and 6 nm, respectively. Fluorescence and synchronous measurements were performed by using a 1 cm quartz cell on a JASCO FP 6600 spectrofluorometer.

4.4 Evaluation of antioxidant assays

4.4.1 DPPH radical scavenging activity

The potential antioxidant activity of ligands and new palladium(II) complexes (**1-4**) was evaluated by diphenyl-1-picrylhydrazyl (DPPH) radical scavenging assay was determined by szabo method.[3]DPPH free radicals are used for rapid analysis of antioxidants. While scavenging the free radicals, the antioxidants donate hydrogen and form a stable DPPH molecule. Briefly, the various concentrations of the complexes (20-100 μg/ml) in 1 ml of 10 % aqueous DMSO were added to 5 ml of DPPH (0.1 mM in methanol) and were mixed rapidly. A negative control was prepared by adding 100 μl of 10% aqueous DMSO in 5 mL of 0.1 mMmethanolic solution of DPPH. Radical scavenging capacity was measured in 10 min intervals using spectrophotometer by monitoring the decrease in absorbance at 517 nm. The IC_{50} values of DPPH decolonization of the complexes were calculated. Ascorbic acid was used as a positive control.

4.4.2 Superoxide anion scavenging activity

The superoxide anion scavenging activity of the new palladium(II) complexes were based on the Liu method.[4]Superoxide radicals were generated in PMS(phenazinemethosulphate)-NADH systems by oxidation of NADH and assayed by the reduction of nitrobluetetrazolium (NBT). 3 ml of sample solutions at different concentrations (20-100 μg/ml) were mixed with 1 ml of NBT (156 μM) and 1 ml of NADH (468 μM). The reaction was initiated by adding

0.1 ml of phenazinemethosulphate (PMS) solution (60 µM) to the mixture. The reaction was incubated at 25 ºC for 5 min, and the absorbance at 560 nm was measured against blank. Decreased absorbance of the reaction mixture indicates increased super oxide anion scavenging activity. Butylatedhydroxy toluene (BHT) was used as the standard.

4.4.3 Reductive ability

The reducing ability of the compounds has been investigated using the Oyaizu method.[5]The various concentrations (20-100 µg/ml) of the complexes in 1 ml of 10% DMSO were mixed with 2.5 ml of phosphate buffer (0.2 mol/l, pH 6.6) and 2.5 ml of potassium ferricyanide (1%). The mixture was incubated at 50 ºC for 20 min. To this solution 2.5 ml of trichloroacetic acid (10% TCA) was added to the mixture and centrifuged at 3000 rpm for 10 min. The supernatant (5 ml) was mixed with 1 ml of ferric chloride (0.1%) and the absorbance was measured at 700 nm in a Spectrophotometer. Increased absorbance of the reaction mixture indicated increased reducing power. Mean value from three independent experiments was recorded as the reducing power of the compound.

4.4.4 Estimation of total antioxidant capacity

Total antioxidant was determined by phosphomolybdenum method[6] followed by Samples and standard (1 ml) was mixed with 2 ml of reagent solution [ammonium molybdate (4 mM), sodium phosphate (28 mM) and sulphuric acid (0.6 M)]. All the reaction mixtures were incubated at 95 ºC for 90 min. The absorbance was measured at 695 nm. Total antioxidant activity was expressed as the number of equivalent of ascorbic acid (µg/ml AA).

For the above assay, all of the tests were run in triplicate and various concentrations of the compounds were used to fix a concentrations at which the compounds showed in and around 50 % of activity. In addition, the percentage of activity was calculated using the formula: % of suppression ratio = $[(A_0 - A_c)/A_0] \times 100$. A_0 and Ac are the absorbance in the absence and presence of the tested compounds, respectively. The IC_{50} (half maximal inhibitory concentration) is a measure the effectiveness of the substance in inhibiting a specific biological or biochemical function. The 50 % activity (IC_{50}) can be calculated using the percentage of activity. All experimental results were expressed as the mean and (±) standard deviation (SD) of triplicate determinations.

4.5 Antibacterial activity studies

The palladium(II) starting material, Schiff base ligands (H_2L)[1-4] and their new palladium(II) complexes (**1-4**) have been screened for their antibacterial activities against various pathogenic bacteria *Staphylococcus aureus*, *Salmonella typhi*, *Escherichia coli*, *Bacillussubtilis*, *Pseudomonas aeruginosa* and *Klebsiellapneumoniae* by disc diffusion method.[7]The test solutions have been prepared in DMSO. The test organisms were grown on nutrient agar medium in Petri plate. The concentration used in this study is 1mg/ml. The sample solutions were placed on the well cut seeded plates and incubated at 37 °C for 24 h. The diameter (mm) of the inhibition zone around each disc was measured after 24 h. *Streptomycin* was used as standard.

4.6 Cytotoxicity studies

4.6.1 3-(4,5-Dimethylthiazol-2-yl)-2,5-diphenyltetrazolium bromide (MTT) assay[8]

MTT, upon reduction by NAD(P)H-dependent cellular oxidoreductase enzymes present in the cytoplasm of metabolically active cells, forms formazan as a purple insoluble product. The amount of formazan estimated by a spectral method correlates with the number of live cells and provides a quantitative measurement of the cytotoxicity of the compound. The IC_{50} values were obtained from nonlinear regression using GraphPad Prism 5.[9] About 6000 cells of MCF-7 (human breast cancer cells) and HeLa (human cervical cancer cells) were taken in each well of a 96-well culture plate and incubated for 24 hours in a CO_2 incubator. After incubation, different concentrations (100, 50, 25, 12.5, 6.25, 3.12 μM) of the compounds dissolved in DMSO were added to the cells. After appropriate incubation time (24 h for complexes, metal percursors, ligands and 1,2-bis (diphenylphosphino)ethane), the wells were treated with 20μl MTT (5 mg/ml phosphate-buffered saline, PBS) and incubated for 3 h. The purple formazan crystals obtained were dissolved in 200μl DMSO and the absorbance was measured at 570 nm in Molecular Devices Spectra Max M5 plate reader. Data were obtained as the average of three independent sets of experiments, all performed in triplicate for each concentration.[8]

References

1. (a) A. Wolfe, G. H. Shimer and T. Meehan, *Biochemistry,*1987, **26**, 6392-6396. (b) G. Cohen, H. Eisenberg, *Biopolymers,* 1969, **8**, 45-55.

2. S. Sathiyaraj, K. Sampath, R. J. Butcher, R. Pallepogu and C. Jayabalakrishnan, *Eur. J. Med. Chem.*,2013, **64**, 81-89.
3. M. R. Szabo, C. Idtoiu, D. Chambre and A. X. Lupea, *Chemistry and Materials science,*2014, **61**, 214-216.
4. F. Liu, V. E. C. Ooi and S. T. Chang, *Life Sci.,*1997, **60**, 763-771.
5. M. Oyaizu, *Jap. J. Nutr.*,1986, **44**, 307-315.
6. P. Prieto, M. Pineda and M. Aguilar, *Anal. Biochem.,*1999, **269**, 337-341.
7. A.W. Bauer, W. M. M. Kirby, J. C. Sherris and M. Turck, *Am. J. Clin. Path.,*1966, **45**, 493-496.
8. T. Mossman, *J. Immunol. Methods*,1983, **65**, 55-63.
9. H. J. Motulsky, Prism 5 Statistics Guide, GraphPad Software Inc., San Diego, CA 2007 http://www.graphpad.com.

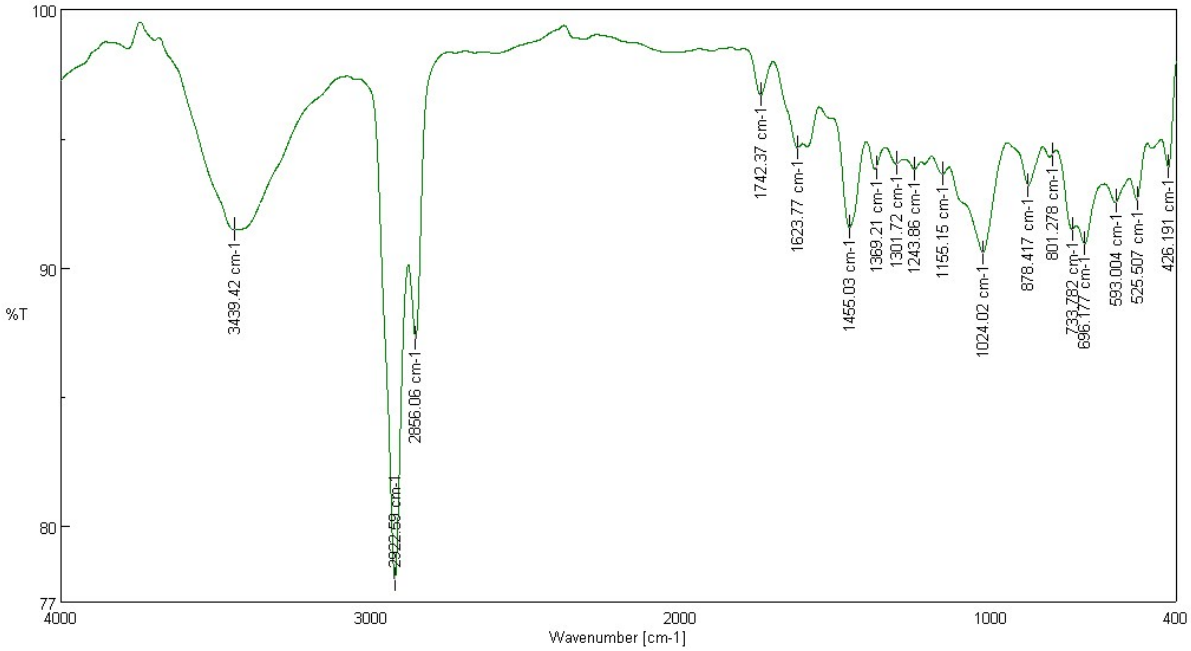

Fig. S1. IR spectrum of $[(Pd_2(Msal\text{-}tsc)_2)(\mu\text{-}dppe)]$ **(1)**

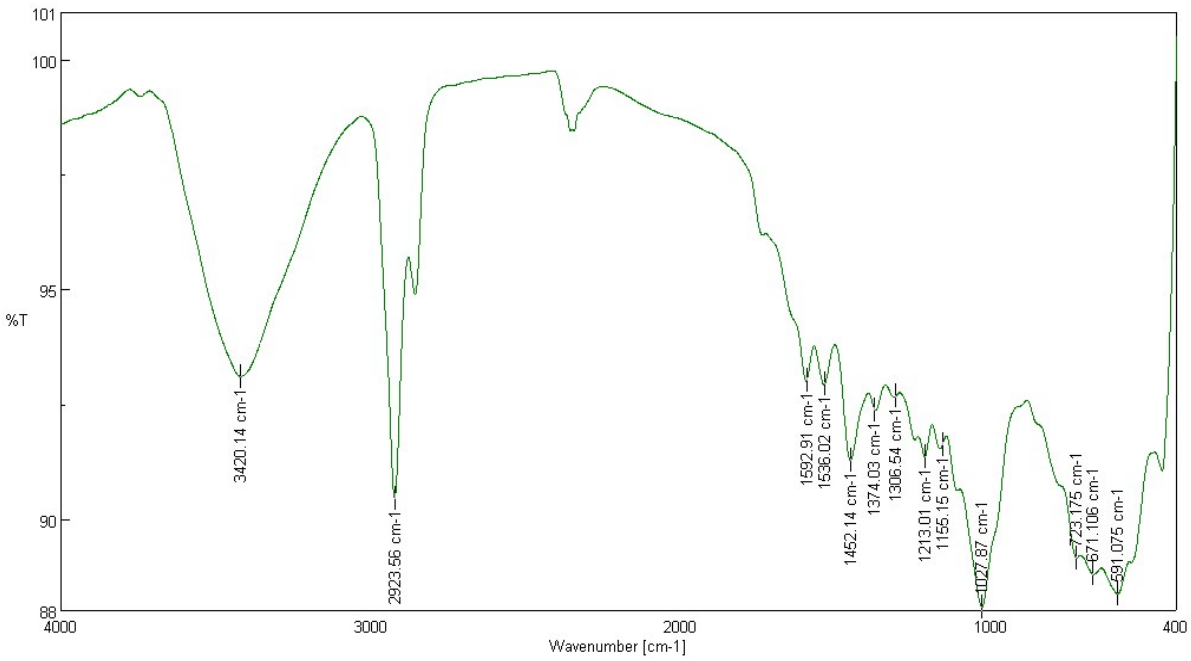

Fig. S2. IR spectrum of [(Pd_2(Msal-mtsc)$_2$)(μ-dppe)] **(2)**

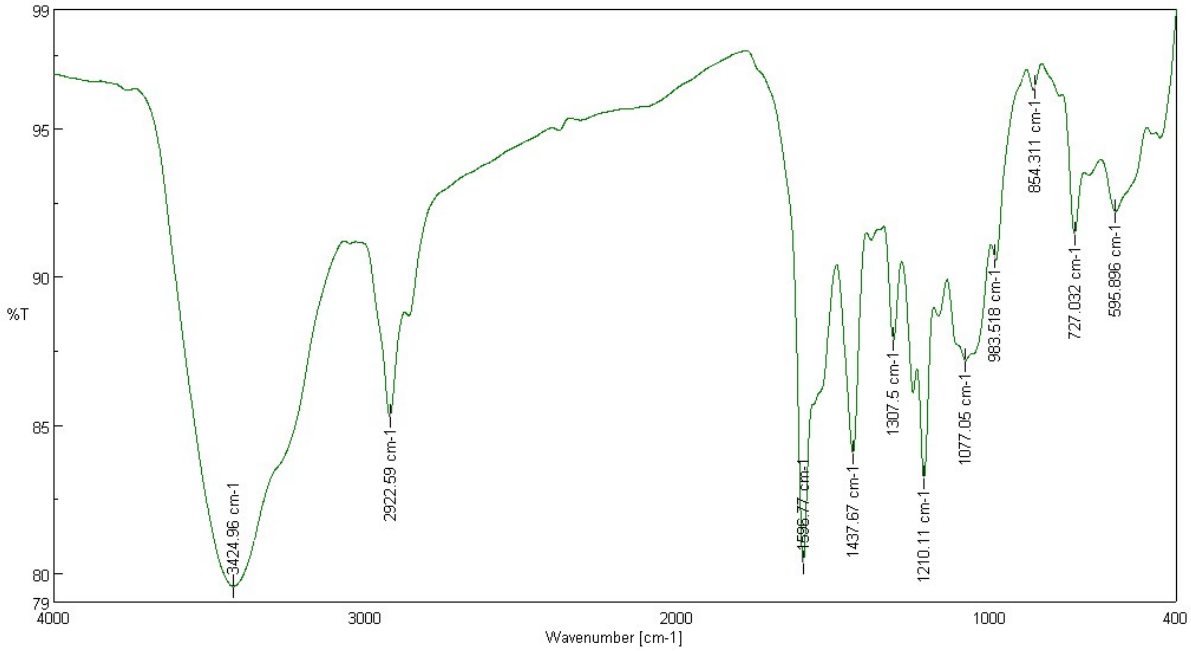

Fig. S3. IR spectrum of [Pd_3(μ-S-Msal-etsc)$_3$]**(3)**

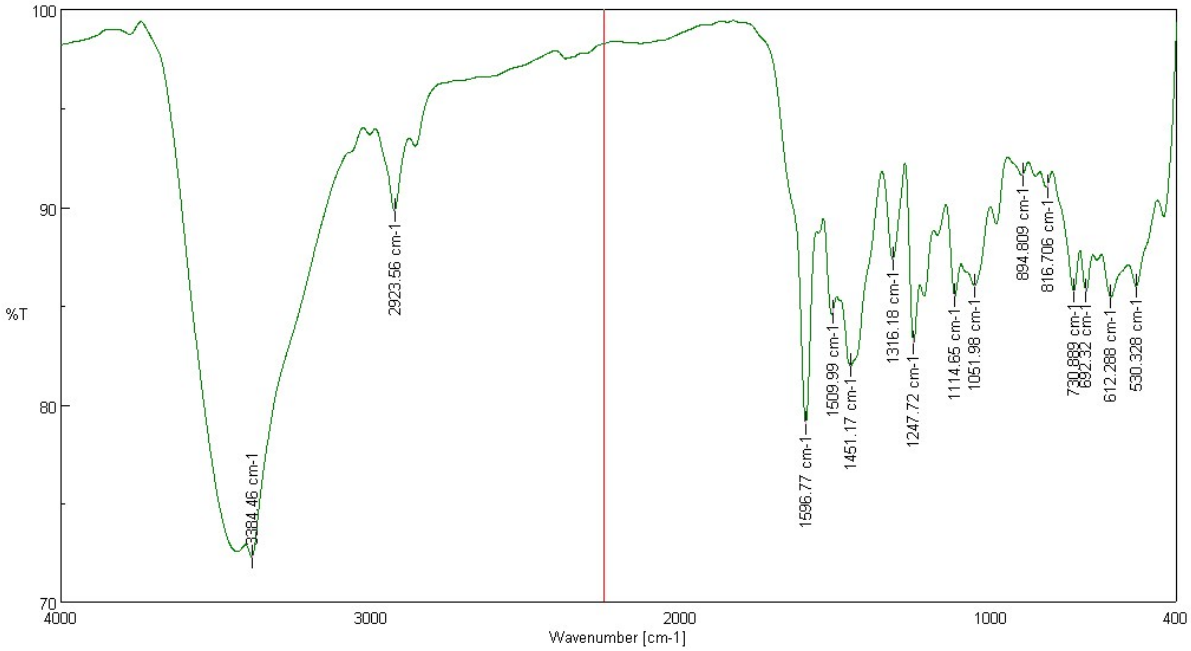

Fig. S4. IR spectrum of [Pd(Msal-ptsc)(Msal-ptaz)] (**4**)

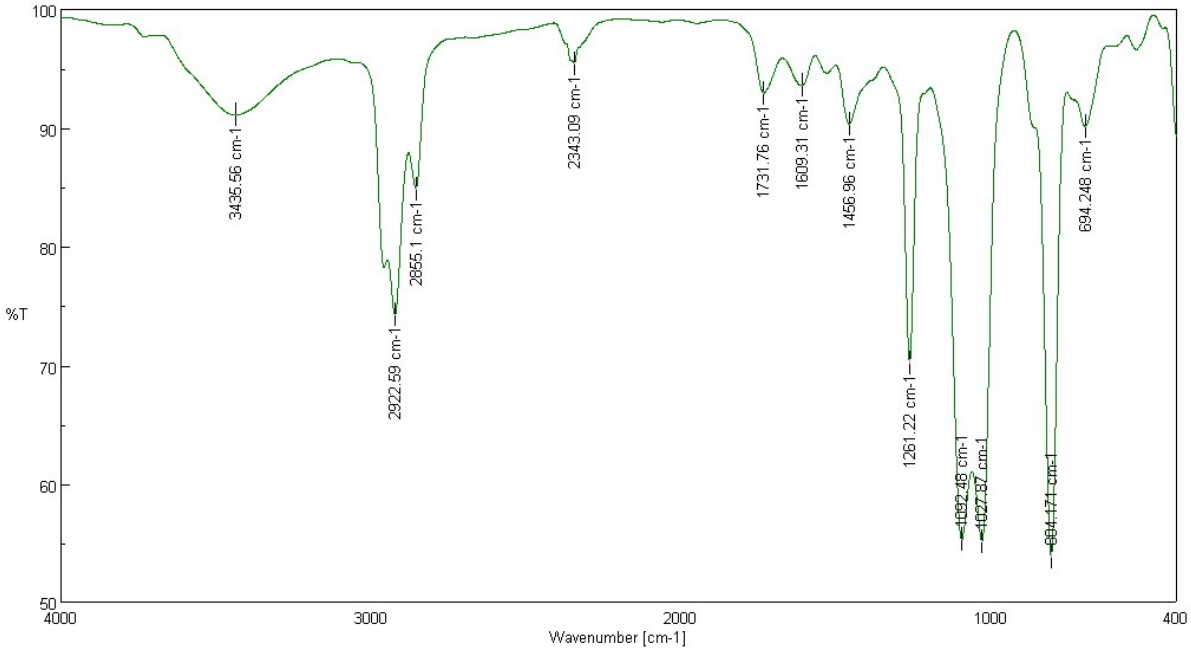

Fig. S5. IR spectrum of [$PdCl_2$(dppe)] **(3a** and **4a)**

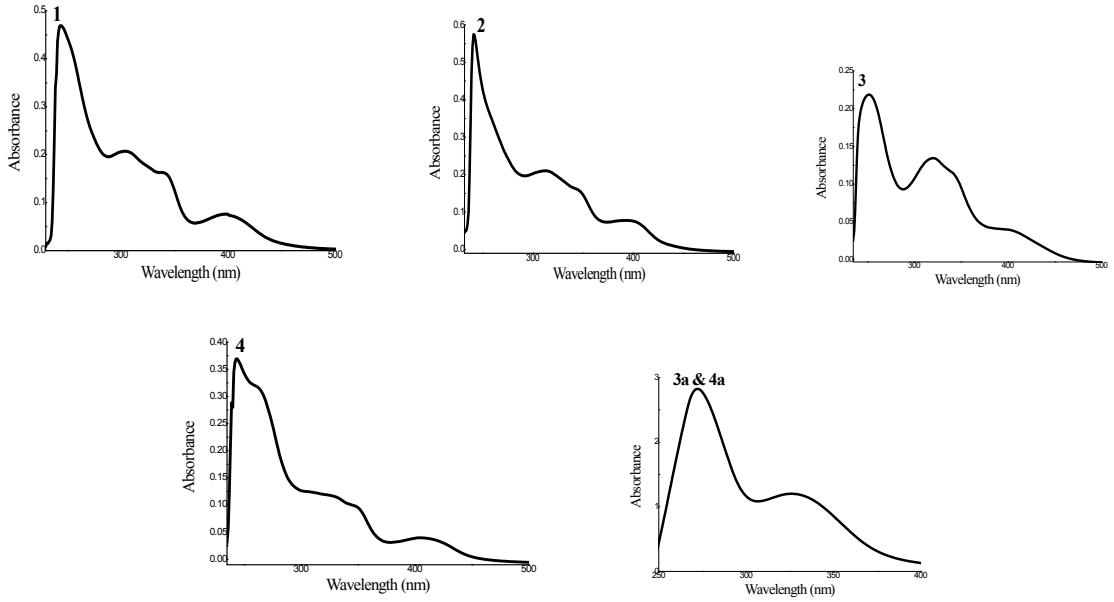

Fig. S6. Electronic spectra of the complexes (**1-4a**)

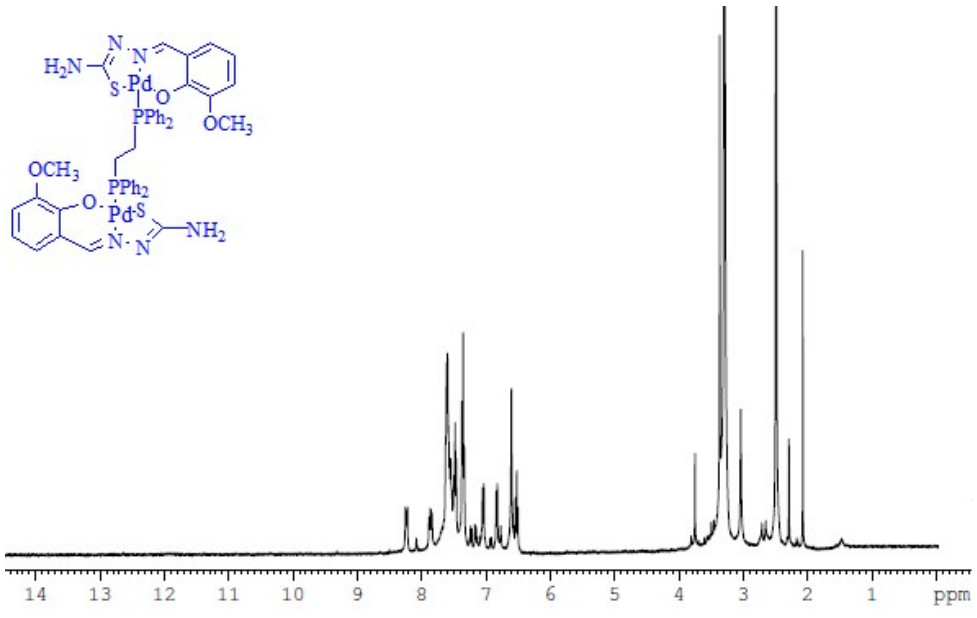

Fig.S7. ^{1}H-NMR spectrum of [(Pd_2(Msal-tsc)$_2$)(μ-dppe)] **(1)**

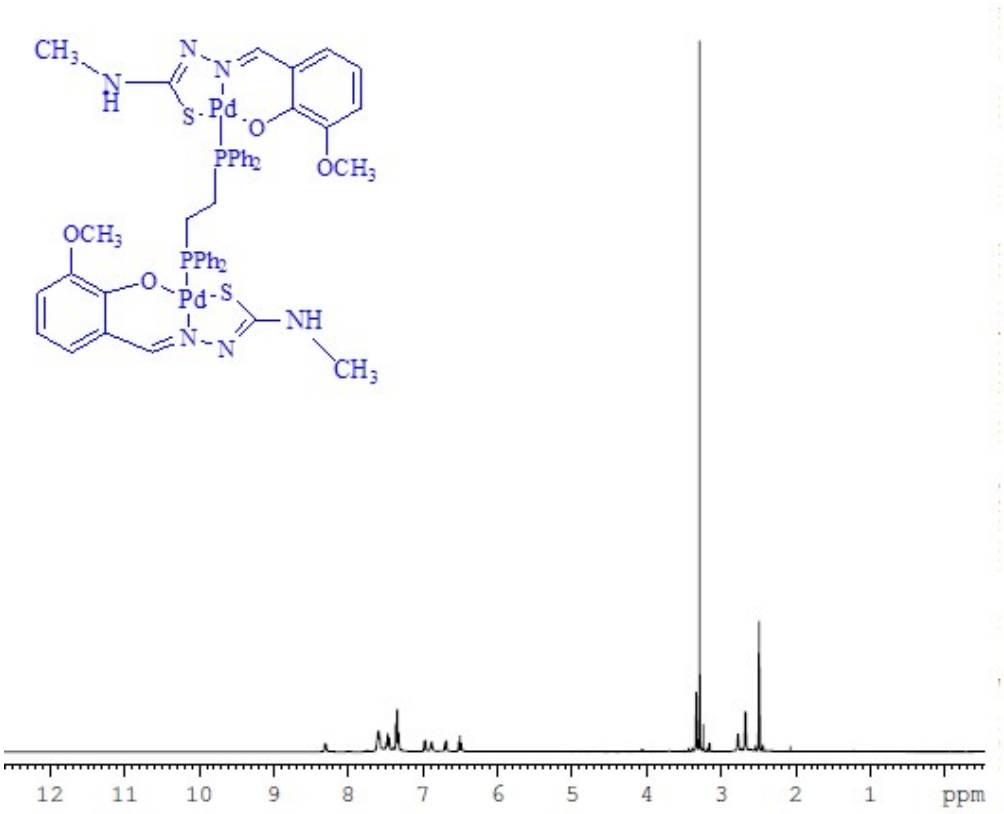

Fig.S8. ^{1}H-NMR spectrum of [(Pd_2(Msal-mtsc)$_2$)(μ-dppe)] **(2)**

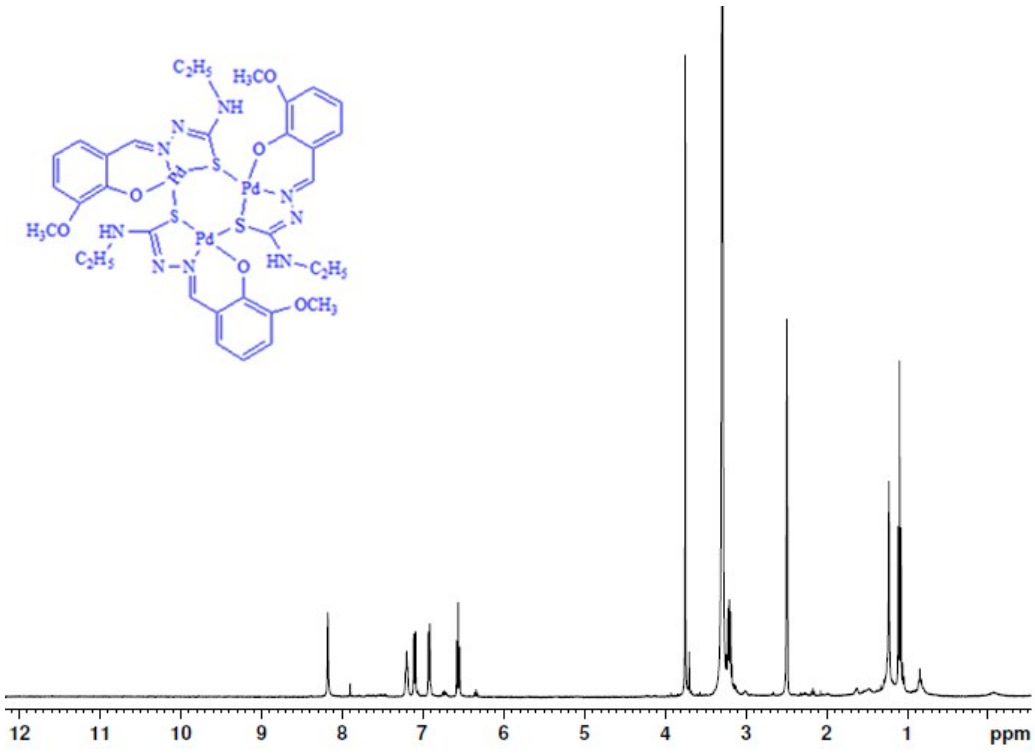

Fig.S9. ^{1}H-NMR spectrum of [Pd_3(μ-S-Msal-etsc)$_3$]**(3)**

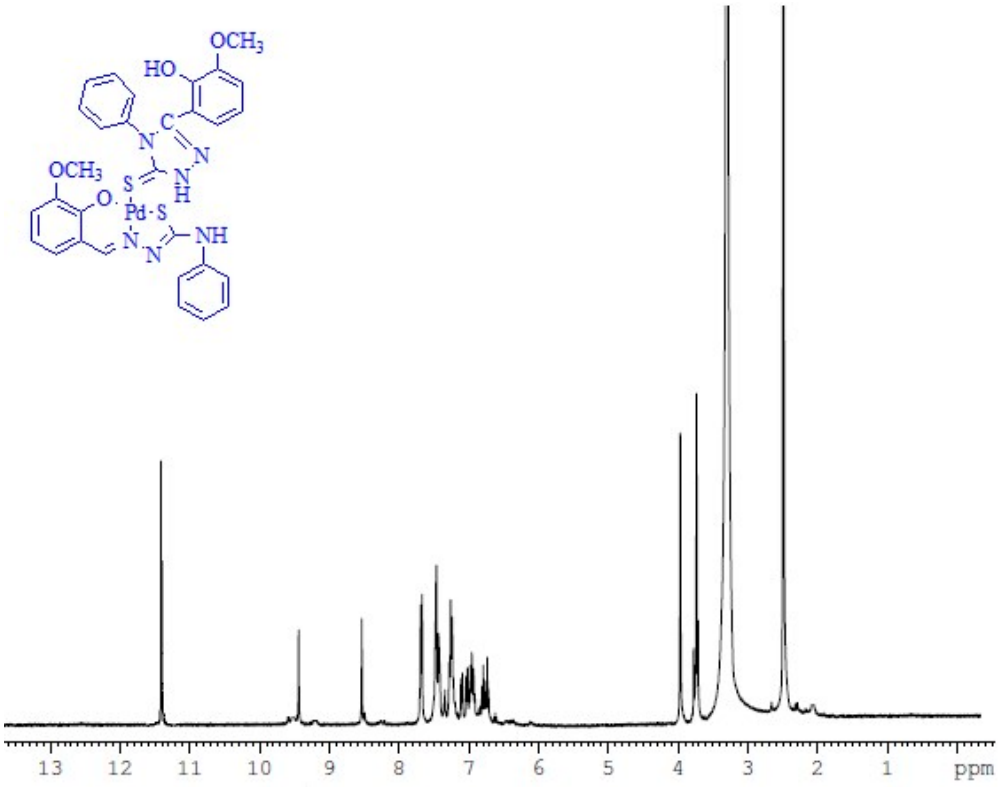

Fig. S10.[1]H-NMR spectrum of [Pd(Msal-ptsc)(Msal-ptaz)] (**4**)

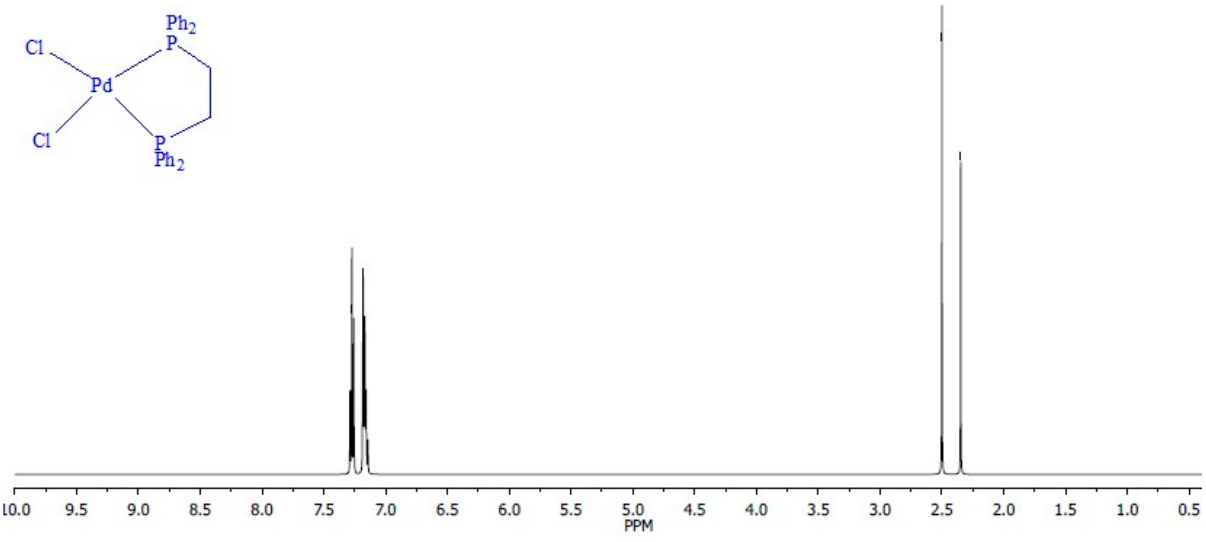

Fig. S11. [1]H-NMR spectrum of [$PdCl_2$(dppe)] **(3a** and **4a)**

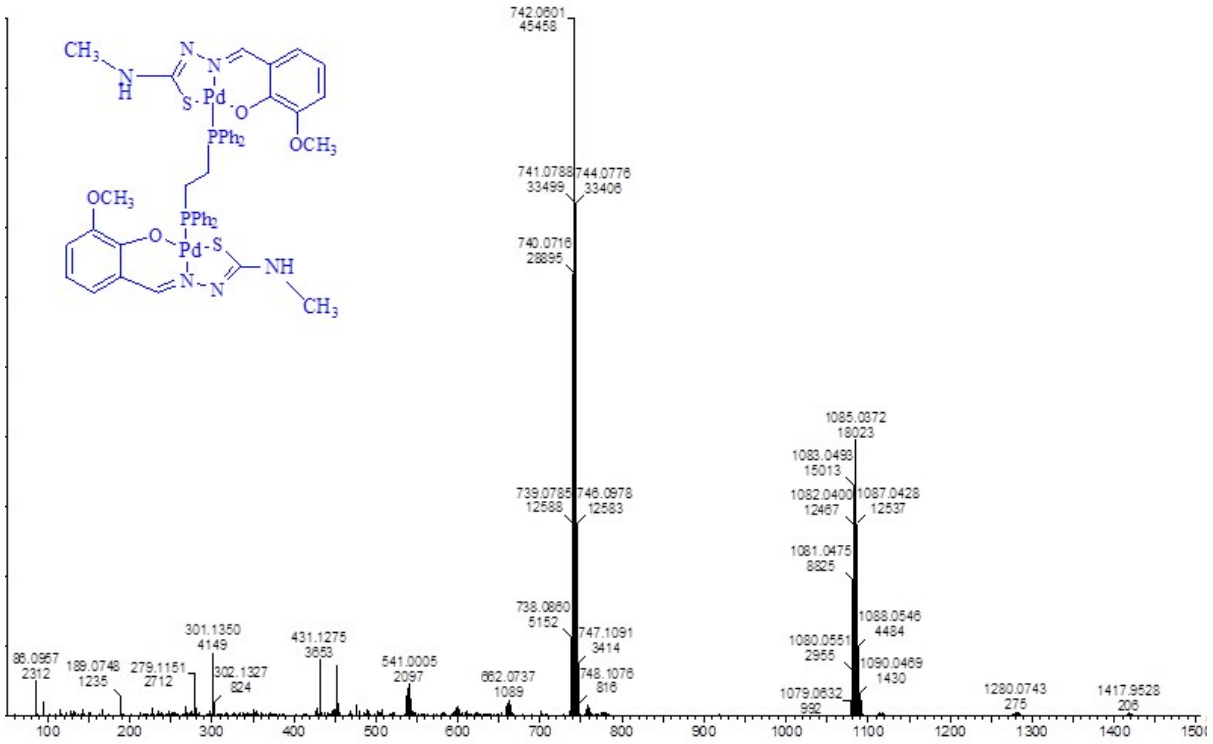

Fig.S12.ESI-MS spectrum of [(Pd_2(Msal-mtsc)$_2$)(μ-dppe)](**2**)

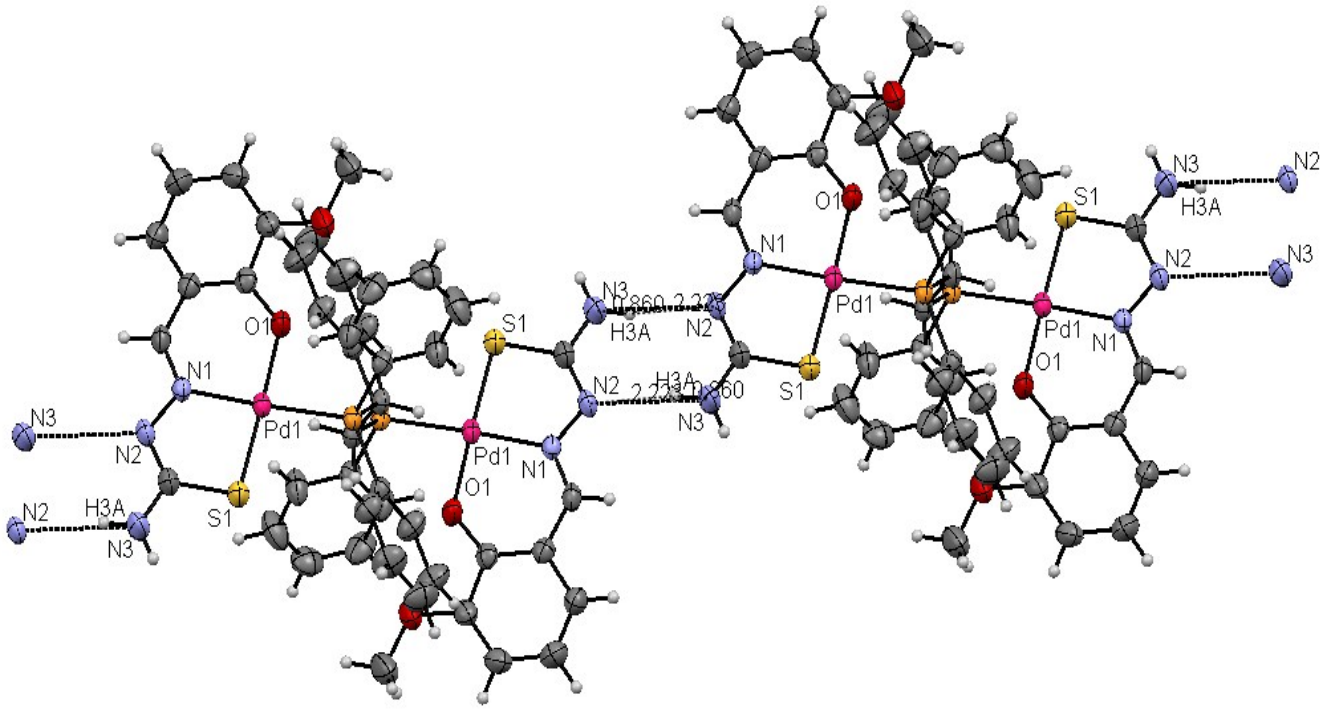

Fig. S13.ORTEP diagram of complex **1** with hydrogen bonding.

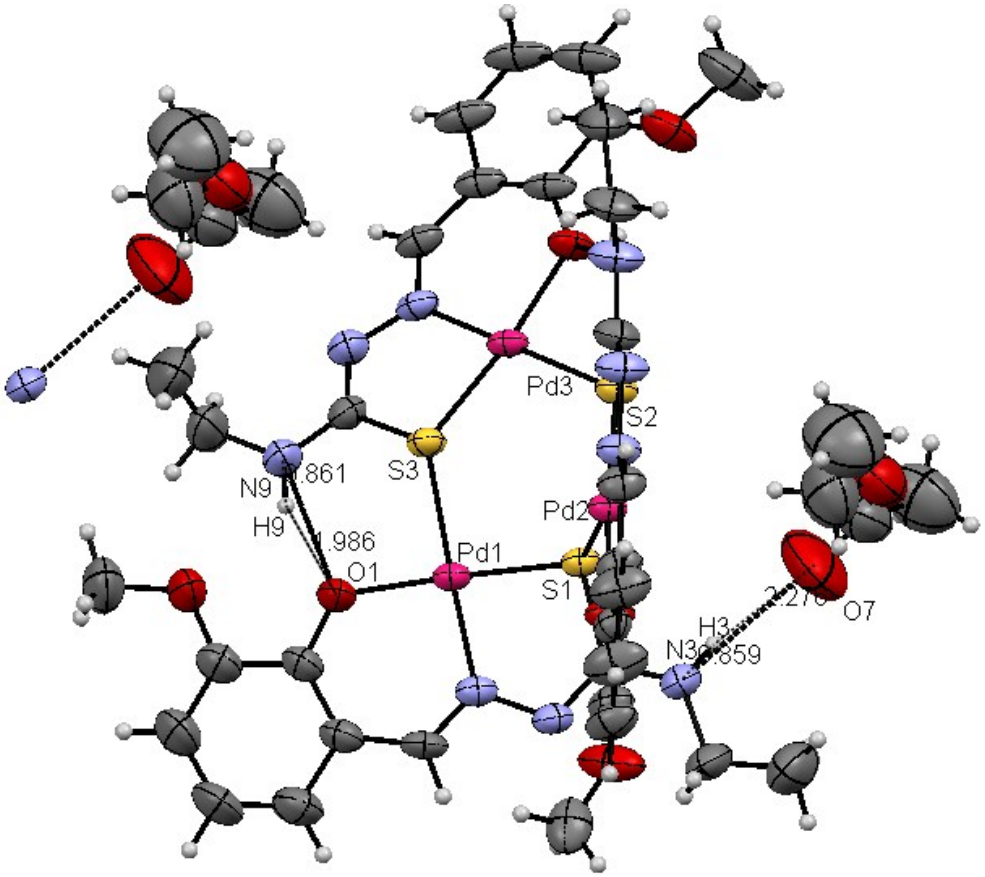

Fig.S14.ORTEP diagram of complex **3** with hydrogen bonding.

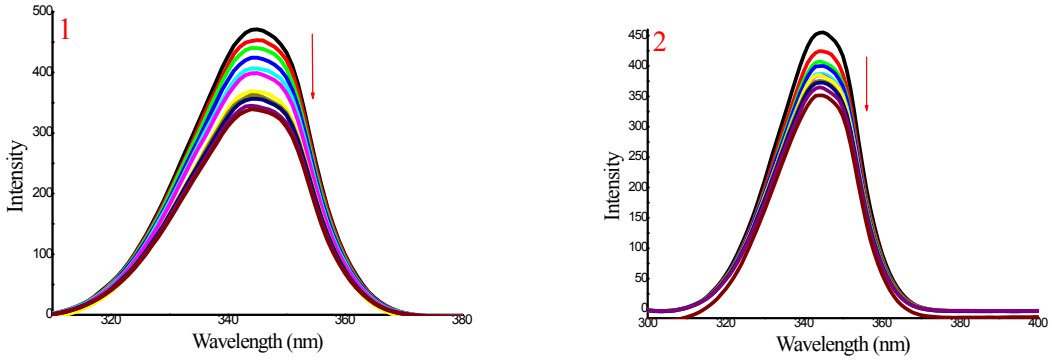

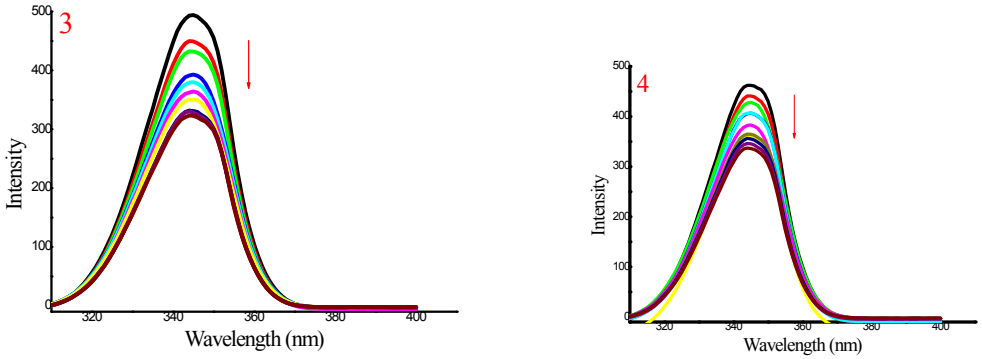

Fig.S15. Synchronous spectra of BSA (1×10^{-6}M) in the absence and presence of complexes **1-4** (0-100 μM) in the wavelength difference of $\Delta\lambda$ = 60 nm.

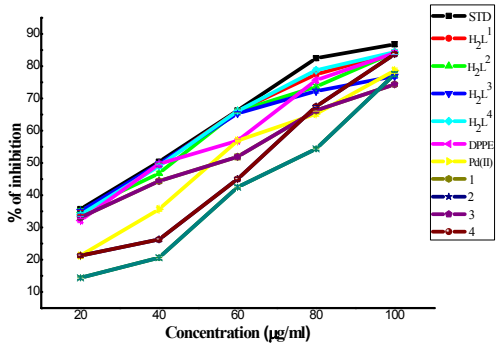

Fig.S16.DPPH scavenging activity of ligands, bis(diphenylphosphino)ethane, $K_2[PdCl_4]$ and new Pd(II) complexes.Errorbarsrepresent the standard deviation of the mean (n=3)

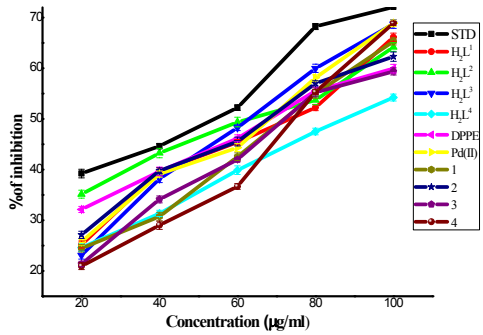

Fig.S17. Superoxide scavenging activity of ligands, bis(diphenylphosphino)ethane, $K_2[PdCl_4]$ and new Pd(II) complexes. Error bars represent the standard deviation of the mean (n=3).

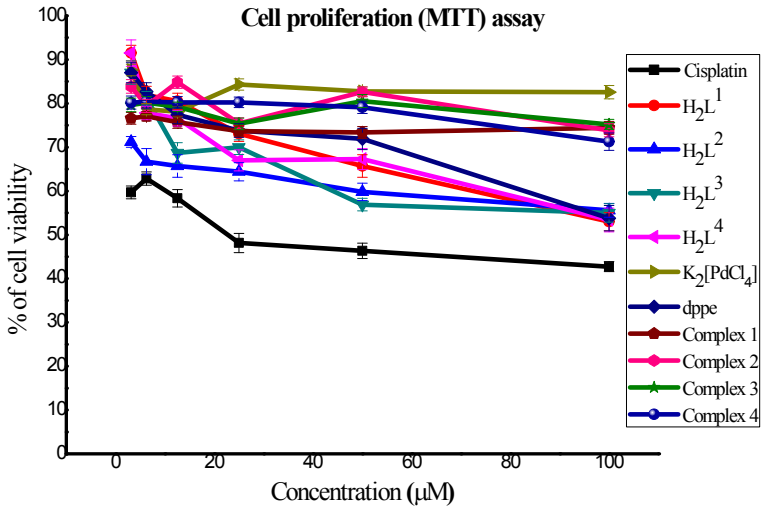

Fig. S18. HeLa cells were treated with different concentrations of complexes **1-4**, ligands, bis(diphenylphosphino)ethane, $K_2[PdCl_4]$ and *cisplatin* (3.125, 6.25, 12.5, 25, 50, 100) for 24 h. cell viability was assessed by cell proliferation (MTT) assay. Error bars represent the standard deviation of the mean (n=3).

Table S1 Crystal data and structure refinement of new Pd(II) complexes

	[(Pd_2(Msal-tsc)$_2$)(μ-dppe)](**1**)	[Pd_3(μ-S-Msal-etsc)$_3$].$C_2H_5COOCH_3$ (**3**)	[Pd(Msal-ptsc)(Msal-ptaz)] (**4**)	[$PdCl_2$(dppe)] (**3a** and **4a**)
Empirical formula	$C_{22}H_{21}N_3O_2PPdS$, 0.5(C_6)	$C_{33}H_{39}N_9O_6Pd_3S_3$	$C_{30}H_{26}N_6O_4PdS_2$	$C_{26}H_{24}P_2PdCl_2$
Formula weight	564.88	1161.21	705.09	577.77
Temperature	293 K	293 K	293 K	293 K
Wavelength	0.71073Å	0.71073 Å	0.71073 Å	0.71073 Å
Crystal system	Triclinic	Triclinic	Monoclinic	Monoclinic
Space group	P-1	P-1	P21/c	P 1 21/c1
Unit cell dimension				
a	10.5318(3)Å	13.2741(3)Å	10.5084(2)Å	11.4546(6)Å
b	11.2368(4)Å	14.1583(3)Å	17.0591(4)Å	13.3176(6)Å
c	11.4307(3)Å	15.4049(4)Å	16.5361(3)Å	16.3164(10)Å
α	93.94º	116.500º	90º	90 º
β	98.609º	92.908º	96.126	98.985 º
γ	107.392º	114.528º	90º	90 º
Volume	1267.08(7)Å^3	2256.02 (10) Å^3	2947.39(11) Å^3	2458.5(2) Å^3
Z	2	2	4	4
Density	1.481 Mg m^{-3}	1.709 Mg m^{-3}	1.589 Mg m^{-3}	1.561Mg m^{-3}
Absorption coefficient	0.904 mm^{-1}	1.380 mm^{-1}	0.819 mm^{-1}	1.095mm^{-1}
F(000)	570	1164	1432	1169
Crystal size	0.18 × 0.09 ×0.05	0.2 × 0.07×0.05 mm	0.17× 0.08×0.08 mm	-

	mm			
Theta range for data collection	3.39 to 29.26º	3.36 to 29.71º	3.40 to 29.72º	3.31 to 28.51º
Index range	13≤ h ≤-13, 15≤ k ≤ -15, 15 ≤ l ≤-15	-17≤ h ≤18, -19≤ k ≤ 18, -21≤ l ≤21	-14≤ h ≤14, -23≤ k ≤ 23, -22≤ l ≤ 22	-11≤ h ≤13, -13≤ k ≤ 17, -19≤ l ≤8
Reflection collected	9359	16847	13206	2674
Completeness to theta	26.32 º	26.32º	26.32º	24.66º
Refinement method	Full-matrix least-square on F^2	Full-matrix least-square on F^2	Full-matrix least-square on F^2	Full-matrix least-square on F^2
Data/restraints/ parameters	6263/1/300	11417/2/557	7536/0/391	4055/0/280
Goodness of fit on F^2	1.042	1.052	1.047	0.966
Final R indices[I>2σ(I)]	R1= 0.0525, WR2 = 0.0942	R1= 0.0667, WR2= 0.0893	R1= 0.0542, WR2= 0.0715	R1= 0.0538, WR2= 0.0761
R indices (all data)	R1 = 0.0391, WR2 = 0.1018	R1= 0.0430, WR2= 0.1019	R1= 0.0351, WR2= 0.0797	R1= 0.0356, WR2= 0.0893

Table S2a Selected bond lengths (Å) and angles (º) of new Pd(II) thiosemicarbazone complex (**1**)

(**1**)			
Bond lengths		**Bond angles**	
Pd1-O1	2.008(2)	O1-Pd1-N1	93.85(9)
Pd1-N1	2.023(2)	S1-Pd1-P1	97.58(3)
Pd1-S1	2.233(8)	N1-Pd1-S1	84.47(7)
Pd1-P1	2.267(7)	O1-Pd1-P1	84.12(6)
		N1-Pd1-P1	177.52(1)
		O1-Pd1-S1	178.29(6)

Table S2b Selected bond lengths (Å) and angles (º) of new Pd(II) thiosemicarbazone complex (**3**)

(**3**)			
Bond lengths		**Bond angles**	
Pd1-O1	2.013(3)	S1-Pd1-S3	94.80(3)
Pd1-N1	1.994(3)	O1-Pd1-S3	87.80(8)
Pd1-S1	2.238(10)	N1-Pd1-S1	84.46(10)
Pd1-S3	2.336(10)	N1-Pd1-O1	92.84(12)
Pd2-O3	2.003(3)	O1-Pd1-S1	177.18(9)
Pd2-N4	1.988(3)	N1-Pd1-S3	173.77(9)
Pd2-S2	2.230(10)	S2-Pd2-S1	89.85(3)
Pd2-S1	2.319(9)	O3-Pd2-S1	91.83(8)

Pd3-O5	2.014(3)	N4-Pd2-S2	84.48(9)
Pd3-N7	1.992(3)	N4-Pd2-O3	94.35(12)
Pd3-S2	2.314(10)	O3-Pd2-S2	174.62(9)
Pd3-S3	2.244(10)	N4-Pd2-S1	171.62(10)
		S3-Pd3-S2	96.74(3)
		O5-Pd3-S2	85.52(9)
		N7-Pd3-S3	84.29(10)
		N7-Pd3-O5	93.99(12)
		O5-Pd3-S3	171.22(9)
		N7-Pd3-S2	176.35(9)
		Pd1-S1-Pd2	95.56(3)
		Pd2-S2-Pd3	117.53(4)
		Pd3-S3-Pd1	127.34(4)

Table S2c Selected bond lengths (Å) and angles (°) of new Pd(II) thiosemicarbazone complexes (**4**) and (**3a** and **4a**)

(**4**)		(**3a** and **4a**)	
Bond lengths		**Bond lengths**	
Pd1-S1	2.232(7)	Pd1-P8	2.235(10)
Pd1-S2	2.316(6)	Pd1-P11	2.237(11)
Pd1-O1	2.033(16)	Pd1-Cl30	2.355(11)
Pd1-N1	1.991(18)	Pd1- Cl31	2.361(12)
Bond angles		**Bond angles**	
S1-Pd1-S2	85.90(2)	P8-Pd1-P11	85.88(4)
O1-Pd1-S2	96.80(5)	P8-Pd1-Cl30	90.05(4)
N1-Pd1-S1	84.73(6)	P11-Pd1-Cl31	90.85(4)
N1-Pd1-O1	92.61(7)	Cl30-Pd1-Cl31	93.44(5)
O1-Pd1-S1	176.81(5)	P8-Pd1-Cl31	172.35(4)
N1-Pd1-S2	170.54(6)	P11-Pd1-Cl30	175.43(4)

Table S3. Hydrogen bonds for complexes **1** and **3** [A˚ and °]

D–H···A	d(D–H)	d(H···A)	d(D···A)	<(DHA)
[(Pd_2(Msal-tsc)$_2$)(μ-dppe)] (**1**)				
N(3)-H(3A)...N(2)	0.860	2.223	3.056	162.8
Symmetry operation: (x, y, z); (-x,-y, -z)				
[Pd_3(μ-S-Msal-etsc)$_3$] (**3**)				

N(9)-H(9)...O(1)	0.861	1.986	2.791	155.2
N(3)-H(3)...O(7)	0.859	2.276	3.046	162.8
Symmetry operation: (x, y, z); (-x,-y, -z)				